

## Accepted Manuscript

Comparative Analysis of Two Polyethylene Foil Materials for Dew Harvesting in a Semi-arid Climate

J.F. Maestre-Valero, V. Martínez-Alvarez, A. Baille, B. Martín-Górriz, B. Gallego-Elvira

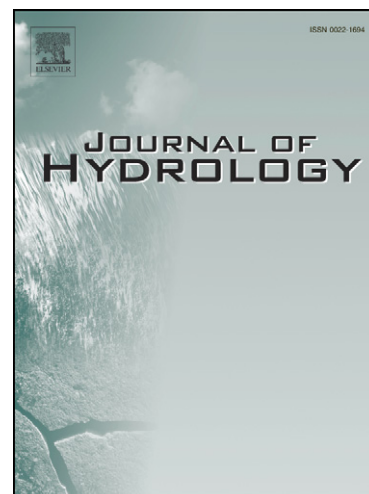
PII: S0022-1694(11)00647-0  
DOI: [10.1016/j.jhydrol.2011.09.012](https://doi.org/10.1016/j.jhydrol.2011.09.012)  
Reference: HYDROL 17835

To appear in: *Journal of Hydrology*

Received Date: 5 April 2011  
Revised Date: 23 August 2011  
Accepted Date: 10 September 2011

Please cite this article as: Maestre-Valero, J.F., Martínez-Alvarez, V., Baille, A., Martín-Górriz, B., Gallego-Elvira, B., Comparative Analysis of Two Polyethylene Foil Materials for Dew Harvesting in a Semi-arid Climate, *Journal of Hydrology* (2011), doi: [10.1016/j.jhydrol.2011.09.012](https://doi.org/10.1016/j.jhydrol.2011.09.012)

This is a PDF file of an unedited manuscript that has been accepted for publication. As a service to our customers we are providing this early version of the manuscript. The manuscript will undergo copyediting, typesetting, and review of the resulting proof before it is published in its final form. Please note that during the production process errors may be discovered which could affect the content, and all legal disclaimers that apply to the journal pertain.



1 **Comparative Analysis of Two Polyethylene Foil Materials for Dew Harvesting in a**  
2 **Semi-arid Climate**

3 J.F. Maestre-Valero\*, V. Martínez-Alvarez, A. Baille, B. Martín-Górriz, B. Gallego-Elvira  
4 Universidad Politécnica de Cartagena. Escuela Técnica Superior de Ingeniería Agronómica.  
5 Paseo Alfonso XIII, 48. 30203 Cartagena. Spain.

6 (\*) Corresponding author, Telephone +34 968 32 70 52. Fax +34 968 32 54 33.

7 Email: [josef.maestre@upct.es](mailto:josef.maestre@upct.es)

8 **Abstract**

9 This paper analyses the dew collection performance of two polyethylene (PE) foils in a semi-arid  
10 region (Southern Spain). The dew collecting devices consisted of two commercial passive radiative  
11 dew condensers (RDCs) of 1 m<sup>2</sup> tilted to 30°. They were fitted with two different high-emissivity  
12 PE foils: a white hydrophilic foil (WSF) recommended as standard for dew recovery comparisons  
13 by the International Organization for Dew Utilization (OPUR), and a low-cost black PE foil (BF)  
14 widely used for mulching in horticulture. Dew yield, foil surface temperature and meteorological  
15 variables (air temperature, relative humidity, downward long wave radiation and wind speed) were  
16 recorded hourly during a 1-year period from May-2009 to May-2010. The spectral emissivity of the  
17 foils was determined in laboratory in the range 2.5-25 µm and the radiance-weighted values were  
18 calculated over different intervals, indicating that BF emitted more than WSF, especially in the  
19 range 2.5-7 µm. Dew yield was well correlated with the air relative humidity and foil net radiation  
20 in both foils and was hardly detected when the relative humidity was lower than 75% or the wind  
21 speed higher than 1.5 m s<sup>-1</sup>. WSF was more sensitive to dew formation due to its hydrophilic  
22 properties, registering more dewy nights (175) than BF (163) while the annual cumulative dew  
23 yield for BF was higher (20.76 mm) than for WSF (17.36 mm) due to the higher emissivity and  
24 emitted radiance of BF. These results suggested that increasing the surface emissivity over the  
25 whole IR spectrum could be more effective for improving RDC yield performances than increasing  
26 the surface hydrophilic properties. On a practical point of view, BF could be considered as a

27 suitable material for large scale RDCs, as in our study it presented several advantages over the  
28 reference material, such as higher dew collection performance, longer lifespan and much lower cost.

29

30 **Keywords:** Water condensers, water harvesting, dew collection, infra-red emissivity, dew  
31 applications.

32

### 33 **1. Introduction**

34 Dew is atmospheric humidity that is transformed into liquid water by passive radiative cooling  
35 (Monteith, 1957; Beysens, 1995; Agam and Berliner, 2006). Under natural conditions, this potential  
36 water source can be widely used by plants and animals in dry environments and can supply enough  
37 moisture to microorganisms for survival (Steinberger et al., 1989; Kidron et al., 2002). Dew  
38 collection by means of manufactured structures could serve as a welcome supplementary source of  
39 water when other sources, such as rain and groundwater are very scarce. Besides, dew could be  
40 used as potable water for human consumption in regions where the water accessibility and supply  
41 becomes difficult (Muselli et al., 2006a; Lekouch et al., 2010), such as semiarid and arid  
42 geographical settings and small islands in developing countries (Beysens et al., 2007; Sharan,  
43 2007a).

44 The essential role of dew as a water source in arid environments, ecosystems and agrosystems  
45 largely explains the increasing interest among scientists and engineers in studying the dew  
46 formation phenomenon. The presence/absence of dew can be readily detected by means of wetness  
47 sensors (Richards, 2009). The quantification of dew yield on different types of surface can be  
48 carried out by means of a wide range of methods, such as absorbent material or cloth plates  
49 (Kidron, 2000), microlysimeters (Jacobs et al., 2002), micrometeorological techniques such as the  
50 Bowen ratio energy balance or the eddy-covariance technique (Vermeulen et al., 1997; Moro et al.,  
51 2007), and dew-specific collectors, called passive 'radiative dew condensers' (RDCs, Beysens et  
52 al., 2005).

53 Among all these methods, RDCs are likely the most suitable techniques to be used at engineering  
54 applications, as they allow to assess the performance of different types of foils and supporting  
55 structures (shape, tilt, etc.). The International Organization for Dew Utilization (OPUR;  
56 <http://www.opur.fr/>) has widely standardised the characterization of dew collection by establishing  
57 the methodology, instrumentation and data obtained from in-field experimental test studies. This  
58 organization recommends the use of a standard material which is made of a special white low-  
59 density polyethylene (PE) foil, with 5% volume of TiO<sub>2</sub> microspheres (diameter 0.19 µm) and 2%  
60 volume of BaSO<sub>4</sub> microspheres (diameter 0.8 µm) embedded in it. This material provides  
61 hydrophilic properties that low the nucleation barrier at the onset of the condensation process  
62 together with a high emissivity in the near infrared (7-14 µm); two important features that favour  
63 dew formation. More information on this material can be found in Nilsson et al. (1994). From here  
64 on, this specially designed white foil is named WSF (White Standard Foil).

65 Several recent investigations aimed to assess the potential for dew harvesting using the standard foil  
66 have been reported. Muselli et al. (2002) tested a 30 m<sup>2</sup> RDC near Ajaccio (Corsica, France),  
67 measuring 214 dewy nights over an observation period of 478 days, with an average of 0.12 mm per  
68 dewy night and a maximum daily yield of 0.38 mm. In a posterior study at the same site (Muselli et  
69 al., 2006a), similar dew yield were obtained (average of 0.13 mm per dewy day). Jacob et al. (2008)  
70 compared two types of RDCs fitted with WSF, one being a 1 m<sup>2</sup> insulated planar dew condenser set  
71 at a 30° angle from horizontal, and the other presenting an inverted-pyramid shape. Recently,  
72 Muselli et al. (2009) studied the dew yield at the Dalmatian Coast with two 1 m<sup>2</sup> RDCs fitted with  
73 WSF, concluding that it could be worthwhile to rehabilitate the numerous deserted rain collectors  
74 (impluviums) existing in the region for the objective of dew harvesting.

75 The standard WSF is currently rather expensive (8\$ m<sup>-2</sup>) since it is generally manufactured for  
76 research purposes. A trend to use low-cost collector foils with similar performances would be  
77 feasible for large scale dew recovery systems, where water can be harvested for domestic and rural  
78 activities at the individual farm or village scale. Some rural development projects, especially in  
79 India (Sharan, 2007a), tried to promote rain and dew recollection over large areas, by covering the

80 soil of gentle-slop terrain with PE foils. In such large scale systems, the covering material should be  
81 of low cost, resistant to weathering, tensile and friction forces, and easily available to farmers of  
82 developing countries. A suitable choice might be the installation of black PE foils that are widely  
83 used in agriculture as soil mulching for weed control, as such films respond to the above criteria.  
84 However, the potential for dew recovery of such films is not known, and need to be assessed before  
85 recommending them for dew harvesting.

86 The main objectives of this study were (1) to compare the properties and dew recovery  
87 performances of a low-cost black PE foil with respect to the standard white PE foil, (2) to analyze  
88 the physical factors driving dew formation to contribute to a better knowledge of the dew formation  
89 process in semi-arid regions and (3) to assess the potential of dew recovery in a semi-arid region of  
90 South Spain, where techniques of dew harvesting could help in mitigating the impact of extreme  
91 drought events.

92

## 93 **2. Materials and Methods**

### 94 **2.1. Site and dew water condensers**

95 The experimental site is located at the Agricultural Experimental Station of the Technical  
96 University of Cartagena, south-eastern Spain (37°41'20" N, 0°57'03"W). This area is characterized  
97 by a Mediterranean semiarid climate with warm, dry summers and mild winters. Average annual  
98 temperature is 17.5 °C, reaching maximum temperatures of 38 °C in summer and minimum  
99 temperatures of 0 °C in winter. Annual rainfall averages 320 mm, with high seasonal and inter-  
100 annual variability. Most precipitation occurs during the fall and winter months, but inter-annual  
101 droughts are also common. Average reference evapotranspiration, calculated by the Penman-  
102 Monteith method (Allen et al., 1998), is about 1,250 mm year<sup>-1</sup>.

103 Two RDCs were set up following the OPUR international standard procedure (Fig. 1). They  
104 consisted of 1 m<sup>2</sup> insulated flat pans tilted 30° to horizontal to ensure a good compromise between  
105 radiative energy loss and water recovery by gravity (Beysens et al., 2003). The water condensing on

106 the surface at night was collected under gravity flow by a gutter and run to a container where it was  
 107 stored and weighed. Both containers were provided with a siphon system for auto-emptying when  
 108 full. One of the RDCs was dressed with the white standard foil (WSF), previously described,  
 109 whereas the other was fitted with a 0.15 mm thick black low-density PE foil (in the following, BF),  
 110 typically used as soil mulching in agriculture. This is a low-cost PE foil (0.8 \$ m<sup>-2</sup>) which is made  
 111 of 97.5% of low density PE, 2.5% of black of carbon and contains some antioxidant and thermal  
 112 stabilizer additives.

113

114 Figure 1. View of the two RDCs with the black PE foil (BF) and the white standard foil (WSF) fitted  
 115 to the 30° tilted flat pans.

116

## 117 2.2. IR optical properties and emitted radiance of the foils

118 A spectrophotometer (FT-IR Bruker Vertex 70) was used for determining the spectral distribution  
 119 (every 10 nm) of the absorptivity (= emissivity) and transmissivity of the foils for the mid IR  
 120 spectrum (2.5 to 25 μm), under wet and dry conditions. Wet conditions were obtained by spraying  
 121 water during five minutes on the foil samples. An average spectral curve, representing the mean of  
 122 five repetitions, was calculated for each foil and surface status.

123 For a given wavelength  $\lambda$ , the emitted radiance ( $W$ , energy lost by radiation to the sky) was deduced  
 124 from the Plank's law:

$$125 \quad W = \frac{C_1}{\lambda^5} \frac{1}{\exp\left(\frac{C_2}{\lambda T_f}\right) - 1} \varepsilon \quad (2)$$

126 where  $C_1 = 3.74 \cdot 10^8$  and  $C_2 = 1.44 \cdot 10^4$  are constants,  $\lambda$  is the wavelength,  $\varepsilon$  is the measured  
 127 emissivity of each foil configuration in each 10 nm wavelength interval and  $T_f$  (K) is the surface  
 128 temperature. The calculations of  $W$  were performed with  $T_f = 278$  K, which could be considered as a  
 129 representative value of the foil temperature for dewy nights in the study area.

130  $W$  and  $\varepsilon$  values were integrated over the following wavelength intervals: 2.5-7 $\mu\text{m}$ , 7-14  $\mu\text{m}$  and 14-  
 131 25  $\mu\text{m}$ . The range 7-14  $\mu\text{m}$  was of special interest as it corresponds to the atmospheric window, the  
 132 range considered in previous studies with the standard foil (e.g. Nilsson et al. 1994). The values of  
 133 the emissivity weighed by the emitted radiance for both foils and under dry and wet conditions were  
 134 calculated (Eq. 3) for all spectrum ranges as:

$$135 \quad \varepsilon^* = \frac{\sum \varepsilon_i W_i}{\sum W_i} \quad (3)$$

136 where  $\varepsilon_i$  and  $W_i$  are the emissivity and the emitted radiance, respectively, at wavelength  $\lambda_i$ .

137

### 138 2.3. Climate and dew measurements

139 During the observation period (May-2009 to May-2010) an automated meteorological station  
 140 located at the vicinity of the RDCs provided the meteorological data required for the study. The  
 141 following variables were continuously recorded at 2 m above ground: air temperature ( $T_a$ ) and  
 142 relative humidity ( $RH$ ) (Vaisala HMP45C probe), wind speed ( $U_2$ ) (Vector Instruments A100R  
 143 anemometer) and downward atmospheric radiation ( $L_a$ ) (Kipp & Zonen CGR 3 pyrgeometer).  
 144 Rainfall ( $P$ ) was measured by means of a tipping bucket gauge (Young 52203). Additional data of  
 145 air temperature, relative humidity and wind speed were also collected close to the foils. Two  
 146 infrared radiometers (Campbell Scientific SI – 111) located 30 cm over the foil supplied the foil  
 147 surface temperature,  $T_f$ . Dew point ( $T_{\text{dew}}$ ) was calculated from  $T_a$  and  $RH$ . The net radiation ( $R_n$ )  
 148 during the night was calculated as  $R_n = L_a - L_f$  with  $L_f = \varepsilon^* \sigma T_f^4$ ,  $\varepsilon^*$  being the radiance weighed  
 149 emissivity of the foil (see section Results).

150 For each RDC, dew was collected at night from 20:00 to 8:00. The dew ran along an inclined gutter  
 151 and passed through a plastic pipe into the container where dew was weighed by means of two high  
 152 precision balances (COBOS, D-3000-CBJ; precision = 0.1 g). A wiper was used daily at dawn to  
 153 scrape the extra water that remained on the foils. This quantity was added to the amount recovered  
 154 in the collecting tanks to give the potential dew recovery. Previous analyses of dew collection on  
 155 the foils indicated the scraped fraction represented about 15 and 20% of the total yield for the WSF

156 and the BF respectively, a slightly lower value than the one reported by Muselli et al. (2002). In the  
157 following, the analysis concerns the potential dew recovery, which represents better the intensity of  
158 the condensation process. No damage due to scraping was noted on the foils during the  
159 measurements period. Eventually, dew yield was calculated as the difference between the maximum  
160 and the minimum weight of water recorded during the night.

161 Dew yield data were statistically analysed by means of the statistical software package Statgraphics  
162 Plus (v.5.1), which performs analysis via a variance technique (ANOVA) to detect any significant  
163 differences between the dew yield of both WSF and BF. Tukey's range test at a 95% confidence  
164 level was calculated for comparison between dew yield data. Data from days corresponding to  
165 rainfall events at night were discarded from the data analysis because of the imprecision in  
166 measuring dew amount.

167 All sensors above described were scanned at 10-s interval and averaged hourly whereas the two  
168 precision balances were scanned at hourly interval. All data were recorded by a datalogger (CR1000  
169 Campbell). The sensors and balances were periodically calibrated.

### 171 **3. Results and discussion**

#### 172 **3.1. Spectrometry and radiance analysis.**

173 Figure 2 presents the spectral distribution of the foil emissivity in the range 2.5-25  $\mu\text{m}$  for WSF  
174 (Fig. 2a) and BF (Fig. 2b), under dry and wet conditions. The curves were quite similar over the  
175 considered spectrum, with the exception of the region from 2.5 to 7  $\mu\text{m}$ , where the emissivity of  
176 WSF was significantly lower than that of BF.

177 The emissivity under wet conditions was slightly higher than in dry conditions for both foils. The  
178 averaged emissivity of WSF increased 1.93% and 0.72% in the 2.5-25  $\mu\text{m}$  range and the 7-14  $\mu\text{m}$   
179 range, respectively. The corresponding increases for BF were 0.26% and 0.60%. This result  
180 indicates that dew formation raised slightly the surface emissivity, the effect being more marked for  
181 WSF.



182 Whereas  $\varepsilon$  of both foils was found to be very similar in the range 7-14  $\mu\text{m}$ , there were significant  
183 differences in the lower wavelength interval (2.5-7  $\mu\text{m}$ ) that affected to some extent the emitted  
184 radiance,  $W$  (Fig. 3a-b).

185

186 Figure 2. Distribution of the foil emissivity ( $\varepsilon$ ) for (a) WSF and (b) BF, under dry and wet  
187 conditions in the 2.5-25  $\mu\text{m}$  range. Vertical bars delimit the 7-14  $\mu\text{m}$  region (atmospheric window).

188

189 Figure 3. Distribution of emitted radiance ( $W$ ;  $W\text{ m}^{-2}$ ) in the 2.5-25  $\mu\text{m}$  range according to the  
190 Planck's law assuming a surface temperature of 278 K for (a) WSF and (b) BF under dry and wet  
191 conditions. Vertical bars delimit the 7-14  $\mu\text{m}$  region (atmospheric window).

192

193 Integrating  $W$  over the three sub-ranges supplied useful information on the relative contribution of  
194 each sub-range to the total emitted radiance ( $W_{\text{tot}}$ ) in the 2.5-25  $\mu\text{m}$  range for the two foils under dry  
195 and wet conditions (Table 1). In all cases, the 7-14  $\mu\text{m}$  region accounts approximately for 50% of  
196  $W_{\text{tot}}$ , whereas the lower region and the upper region contributed to 7% and 43%, respectively. Under  
197 dry conditions,  $W_{\text{tot}}$  was higher for BF (267.3  $W\text{ m}^{-2}$ ) than for WSF (262.0  $W\text{ m}^{-2}$ ), that is a  
198 difference of 5.3  $W\text{ m}^{-2}$  which has to be ascribed mainly to the difference of  $W$  in the lower sub-  
199 range (19.4 vs 15.4  $W\text{ m}^{-2}$ ). The trend was similar under wet conditions, but the differences were  
200 somewhat smaller:  $W_{\text{tot}} = 268.5$  and 265  $W\text{ m}^{-2}$  for BF and WSF respectively, a difference of 3.5  
201  $W\text{ m}^{-2}$  which was mainly due to the difference observed in the lower sub-range (19.4 vs 16.1  $W\text{ m}^{-2}$ ),  
202 as for the dry foils. The presence of water on the foil surfaces slightly increased  $W$  in all sub-ranges,  
203 the increase being greater for WSF (+5  $W\text{ m}^{-2}$ ) than for BF (+1.2  $W\text{ m}^{-2}$ ).

204 Water also increased the values of  $\varepsilon^*$ , the emissivity weighed by the emitted radiance for both foils  
205 (Table 1). Among foils, the values of  $\varepsilon^*$  were very similar for the middle and upper sub-ranges, but  
206 presented differences in the lower sub-range. Under dry conditions,  $\varepsilon^*$  in the 2.5-7  $\mu\text{m}$  interval was  
207 equal to 0.825 and 0.995 for WSF and BF respectively. Under wet conditions, the difference was

208 somewhat smaller (0.850 and 0.996 respectively). Considering the whole spectrum range, BF  
209 presented the highest values of  $\varepsilon^*$  under dry (0.985 vs 0.971 for WSF) as well as wet (0.990 vs  
210 0.980 for WSF) conditions. Therefore, it could be recommended to use the radiance-weighted  
211 emissivity  $\varepsilon^*$  for the calculation and simulation of the emitted radiance from dew collecting  
212 surfaces.

213 Summarizing, both foils presented similar values of  $W$ ,  $\varepsilon$  and  $\varepsilon^*$  for  $\lambda > 7 \mu\text{m}$ , but with significant  
214 differences in the range 2.5-7  $\mu\text{m}$ . Accordingly, it can be concluded that BF presents a higher  
215 emissive power than WSF, due to the higher emissivity of BF in the range 2.5-7  $\mu\text{m}$ , although the  
216 lower emissivity of the WSF in the lower spectral range allow to reflect sunlight and also acquire a  
217 role of passive air conditioning if it is applied on roofs. Besides, the higher reflectance of WSF in  
218 the short-wave (solar spectrum) provides lower surface temperature during the day than BF,  
219 resulting in WSF reaching more rapidly the dew-point temperature than BF (Sharan et al., 2007b).

220

221 Table 1. Integrated values of emitted radiance ( $W$ ;  $W m^{-2}$ ), emissivity ( $\varepsilon$ ) and radiance-weighted  
222 emissivity ( $\varepsilon^*$ ) in the 2.5-7  $\mu\text{m}$ , 7-14  $\mu\text{m}$ , 14-25  $\mu\text{m}$  and the entire mid-infrared (MIR) ranges  
223 under dry and wet conditions.

224

### 225 3.2. Foils performance.

226 During the 1-year experimental period, the number of dewy nights amounted to 175 and 163 for  
227 WSF and BF respectively (Table 2). Accounting for the lack of data due to sensor failure for 27  
228 days of the observation period, the frequency of dew was 52% and 48% for WSF and BF  
229 respectively. Rainfall events (50 days) were unevenly distributed throughout the experimental  
230 period, amounting to a total of 490 mm.

231

232 Table 2. Number of dewy, rainfall and sensor failure nights and total monthly dew yield for the  
233 WSF and BF condensers during the observation period.

234

235 Our results showed that dew yield was season-dependent. Three periods differing markedly in dew  
236 yield could be distinguished. The first one ranged from May-09 to July-09, the second one covered  
237 the summer months and the third corresponded to the period October-09 to May-10 (Table 2). The  
238 lowest monthly dew yield was observed in September, for both WSF (0.57 mm, 6 dewy nights) and  
239 BF (0.69 mm, 4 dewy nights), whereas the highest yield occurred in October (values of 3.18 mm  
240 and 3.83 mm for WSF and BF, respectively). The latter could be attributed to (i) strong radiative  
241 cooling at night due to the prevalence of clear sky conditions (only 2 rainfall events in October  
242 against 10 in September), (ii) high atmospheric humidity resulting from the high soil evaporation  
243 rate after heavy rainfalls (276 mm) on late September (Fig. 4) and (iii) low wind speed during the  
244 night. These conditions resulted in that the difference between dew-point and foil temperature  
245 reached its highest values in October.

246 Cumulated dew yield over the observation period was 17.36 and 20.76 mm for WSF and BF  
247 respectively (Fig. 4). The results from the statistical analysis indicated that significant differences  
248 on dew yield were found between both foils, being the BF approximately 15% more efficient in  
249 recovering dew than WSF. The better performance of BF could be ascribed to its higher emissivity  
250 and emitted radiance (Table 1). This finding was confirmed with the nightly value of minimum foil  
251 temperature, which was on average 0.43 °C lower for BF than for WSF.

252

253 Figure 4. Cumulated dew yield of WSF and BF condensers during the observation period. Bars  
254 represent rainfall events (mm).

255

256 The dew yield histogram by classes of 0.05 mm (Fig. 5) suggested that the higher number of dewy  
257 events with low yield (less than 0.05 mm) for WSF were due to its hydrophilic surface properties.  
258 This characteristic allowed WSF to recover water from small events of dew (less than 0.10 mm)  
259 whereas the BF was less effective in this aspect. Conversely, BF was more efficient in the upper  
260 classes due to its higher emissivity. These respective advantages of WSF and BF appear to be of the

261 same magnitude in the dew yield range 0.05- 0.10 mm, where dew yield frequency for the two foils  
 262 was identical (Fig. 5). These results make clear the influence of the dew yield potential in the  
 263 experimental location on the comparison of yield performance between both foils, i.e. if the  
 264 experiment had been carried out in another region characterised by smaller dew yield events (less  
 265 than 0.10 mm), the hydrophilic properties of the WSF had probably allowed the WSF to collect  
 266 more water than the BF. However, under the south-eastern Spain semi-arid conditions the BF has  
 267 clearly better yield performance than the WSF.

268

269 Figure 5. Dew yield frequency histogram of WSF (white bars) and BF (black bars) during the  
 270 observation period.

271

272 In our study, the maximum dew yield recorded during a dewy night was 0.314 mm in December-09  
 273 for WSF and 0.316 mm in October-09 for BF. These values corresponded to the period from  
 274 October-09 to December-09 when clear sky, low wind speed, and high values of atmospheric  
 275 humidity were prevailing. Conversely, the lowest dew yield values for both foils were found during  
 276 the driest months, i.e. July and August 2009 (Table 3). On annual scale, mean values were 0.105  
 277 mm d<sup>-1</sup> and 0.128 mm d<sup>-1</sup> for WSF and BF, respectively (Table 3).

278

279 Table 3. Monthly and annual maximum, average, and standard deviation of dew yield for the WSF  
 280 and BF condensers during the observation period.

281

### 282 3.3. Correlation with meteorological variables

283 The observed night dew yield,  $Y$  (mm night<sup>-1</sup>), was first related to the dew point-to-air difference  $\Delta T$   
 284 =  $T_{\text{dew}} - T_{\text{a}}$  (Fig. 6), that is, with the relative humidity,  $RH$ . The experimental data were fit to the  
 285 following linear relationship to get an estimate of  $Y$ ,  $Y_{\text{est}}$ , from the knowledge of  $\Delta T$ .

286

$$287 \quad Y_{\text{est}} = a_1 (\Delta T - a_2) \quad (3)$$

288

289 where  $a_1$  (in  $\text{mm } ^\circ\text{C}^{-1}$ ) is the dew yield sensitivity to  $\Delta T$  and  $a_2$  the threshold value of  $\Delta T$  below  
 290 which condensation was not observed (Note that the threshold value of RH would be  $\sim 75\%$ , Fig. 6).

291 There were no significant differences in the parameter values between the two foils ( $a_1 = 0.049 \pm$   
 292  $0.0056 \text{ mm } ^\circ\text{C}^{-1}$  and  $a_2 = -4.2 \text{ } ^\circ\text{C} \pm 0.26$  for WSF,  $a_1 = 0.051 \pm 0.0059 \text{ mm } ^\circ\text{C}^{-1}$  and  $a_2 = -4.6 \text{ } ^\circ\text{C} \pm$   
 293  $0.29$  for BF). The dew yield sensitivity was in between the values found by Muselli et al. (2006b)  
 294 and Muselli et al. (2009). Overall, the predictive performance of Eq. 3, characterised by standard  
 295 statistical parameters (see Table 4) could not be considered as satisfactory. The experimental data  
 296 presented considerable scatter over the whole range of  $\Delta T$ , indicating that  $\Delta T$  alone was a poor  
 297 descriptor of dew yield.

298

299 Figure 6. Correlation of dew yield  $Y$  ( $\text{mm night}^{-1}$ ) with  $\Delta T = T_{\text{dew}} - T_a$  ( $^\circ\text{C}$ , lower scale) and relative  
 300 humidity  $RH$  ( $\%$ , upper scale) for WSF (white symbols) and BF (black symbols).

301

302 To refine the correlation analysis, the residuals of Eq. (3) ( $r = Y - Y_{\text{est}}$ ) were calculated and related  
 303 to other climatic variables, revealing that the residuals were mainly dependent on the nightly net  
 304 radiation, for both WSF and BF (Fig. 7).

305

306 Fig. 7. Relationship between the residuals ( $r$ ) of Eq. (3) and the mean nightly net radiation ( $R_n$ ) for  
 307 WSF (white symbols) and BF (black symbols).

308

309 Subsequently, Eq. (3) was multiplied by a function of  $R_n$ ,  $g(R_n)$ , to account for this dependence.

310 After testing various types of function, a decreasing hyperbolic function was found to supply the  
 311 best fit (lowest root mean square error between observed and estimated values). The proposed

312 empirical model to predict  $Y$  from  $T_a$ ,  $T_{\text{dew}}$  and  $R_n$  was:

313

$$314 \quad Y_{est} = f(\Delta T) \quad g(R_n) = (b_1(\Delta T + b_2)) \left(1 + \frac{b_3}{R_n}\right) \quad (4)$$

315

316 with  $b_1 = 0.126$  and  $0.129$ ,  $b_2 = 3.9$  and  $4.1$  and  $b_3 = 19.21$  and  $18.93 \text{ W m}^{-2}$  respectively for WSF  
 317 and BF. The addition of  $R_n$  as supplementary predictive variable improved considerably the  
 318 predictive performance with respect to Eq. (3) (Fig. 8; Table 4).

319

320 Fig. 8. Comparison between observed ( $Y$ ) and estimated ( $Y_{est}$ ) night dew yield, using Eq. (4) (WSF:  
 321 white symbols, BF: black symbols). The dashed line is the 1:1 relationship.

322

323 Table 4. Values of (i) fitted parameters and (ii) statistical parameters characterizing the predictive  
 324 performance for Eqs. 3 and 4

325

326 Using wind speed at 2m ( $U_2$ ) as additional variable to  $\Delta T$  and  $R_n$  improved only marginally the  
 327 predictive performance (results not shown). The distribution of dew yield vs. wind speed (Fig. 9)  
 328 indicated that most of the events of dew occurred when  $U_2$  was lower than  $1 \text{ m s}^{-1}$ .

329

330 Figure 9. Correlation of dew yield with wind speed  $U_2$  and wind speed frequency classes for WSF  
 331 (white symbols) and BF (black symbols). Wind frequency has been only plotted for the range where  
 332 dew formation occurs ( $0$  to  $2 \text{ m s}^{-1}$ ).

333

### 334 3.4. Potential dew yield

335 If  $T_{dew} = T_a$ , Eq. (4) theoretically provides the maximum attainable yield  $Y_{max}$  under our study  
 336 conditions (Fig. 10):

$$337 \quad Y_{max} = 0.49 \left(1 + \frac{19.21}{R_n}\right) \quad \text{and} \quad Y_{max} = 0.53 \left(1 + \frac{18.93}{R_n}\right) \quad (5)$$

338 respectively for WSF and BF. As it could be deduced from the values of  $b_3$  (19.21 for WSF and  
339 18.83 for BF), no condensation would occur for nightly mean values of  $R_n$  higher than  $-20 \text{ W m}^{-2}$ .  
340 The curves indicated a fast increase in dew recovery potential in the range  $-20$  to  $-40 \text{ W m}^{-2}$ . For  $R_n$   
341  $= -100 \text{ W m}^{-2}$ , value that could be considered as the maximum radiative cooling power for a  
342 condenser (Monteith, 1957; Sharan et al., 2007c), the maximum potential yield would be 0.40 and  
343 0.43  $\text{mm night}^{-1}$  for WSF and BF respectively, confirming the slightly higher potential for dew  
344 recovery observed with BF.

345

346 Fig. 10. Maximum dew yield as a function of foil net radiation as predicted from Eq. 5 for WSF  
347 (white symbols) and BF (black symbols).

348

#### 349 **4. Conclusion**

350 RDCs have been demonstrated to serve as a complementary source of drinking water, mainly in  
351 developing countries, rural areas or small islands, where free-access to water and energy is  
352 expensive. In these regions they are ahead of other techniques such as distillation or desalination, or  
353 deep underground water extraction, all of which require a large amount of energy and a massive  
354 infrastructure to operate.

355 Our study under south-eastern Spain semi-arid conditions demonstrated that the potential for dew  
356 yield of a low-cost black PE foil (BF) was slightly higher than that of the OPUR-standard foil  
357 (WSF), although the BF does not present the hydrophilic properties of the latter. This disadvantage  
358 of BF resulted in less dewy days observed, but was more than compensated on the quantitative  
359 aspect - i.e. the amount of annual recollected water - by the higher emissivity and radiative cooling  
360 power of BF in the lower range ( $2.5\text{-}7 \mu\text{m}$ ) of the mid IR spectrum. It should be pointed out that the  
361 hydrophilic properties of WSF might predominate over the higher emissive power of BF in regions  
362 characterised by small dew yield events.

363 Our results suggested that (i) the knowledge of the emissivity in the whole IR spectrum is necessary  
364 to correctly assess the performance of the foil and (ii) ensuring a high emissivity over the whole IR  
365 spectrum appeared more effective for increasing RDC yield than improving surface hydrophilic  
366 properties. On a practical point of view, BF could be considered as a suitable material for large-  
367 scale RDCs, as in our study, it presented several advantages over the standard reference foil, i.e.  
368 higher dew collection performance, longer lifespan and much lower cost. Dealing with the last two  
369 aspects, it must be pointed out that if the WSF were manufactured in large quantities and anti-UV  
370 treated, its cost might be reduced and its lifespan extended.

371 With respect to yield performances, we showed that RDCs installed in semi-arid coastal sites  
372 similar to our study site (Southern Spain) could recollect approximately 20 mm per year. This value  
373 was somewhat higher than those observed in previous studies in other Mediterranean coastal zones  
374 situated more at North, such as Corsica or the Croatian Coast (Muselli et al., 2002; Beysens et al.,  
375 2007; Muselli et al., 2009), but lower than those reported for arid countries such as the Negev,  
376 Israel (Kidron 1999). It should be stressed that the highest values of daily dew yield were observed  
377 mainly during periods following heavy rainfalls, due to high soil evaporation and high nocturnal  
378 atmospheric humidity. Therefore, it is likely that the amount of recollected dew would depend in  
379 part on the importance, frequency and time occurrence of rainfall events that affect the humidity  
380 content of the air at the vicinity of the condenser. This was confirmed by our correlation analysis  
381 between nightly yield and atmospheric variables, where the predominant predictive variables were  
382 found to be the relative humidity and the net radiation of the foil.

383 An empirical relationship between yield and the two mentioned predictive variables was proposed  
384 that explained about two-thirds of the total variance, and could be used to estimate daily dew yield  
385 with reasonable accuracy. From this relationship, it was derived that the potential yield could be,  
386 expressed as a function of  $R_n$  and could reach up to a maximum of  $0.40 \text{ mm night}^{-1}$  under strong  
387 radiative cooling ( $R_n \sim -100 \text{ W m}^{-2}$ ).

388 Finally, it has to be stressed that the foil net radiation is required to predict dew yield with a  
389 reasonable accuracy, implying that the temperature of the foil surface should be either measured or



390 estimated by means of a model describing the energy balance of the surface (Finch et al., 2002).  
391 Such a model would be of paramount interest (i) for assessing the performances of RDCs in  
392 different locations and climates and (ii) in the design of optimal RDC structure, shape and  
393 orientation.

394

### 395 **Acknowledgments**

396 The authors acknowledge the Foundation Seneca (Murcia, Spain) and the Ministry of Science and  
397 Innovation for the financial support of this study through the grants 02978/PI/05 and AGL2010-  
398 15001 respectively.

399

400

401

402

403

404

405

406

407

408

409

410

411

412

413

414 **References**

- 415 Agam, N. and Berliner, P.R., 2006. Dew formation and water vapor adsorption in semi-arid  
416 environments - a review. *Journal of Arid Environments*, 65,572–590.
- 417 Allen, R.G., Pereira, L.S., Raes, D., Smith, M., 1998. *Crop Evapotranspiration. Guidelines for*  
418 *Computing Crop Water Requirements. Irrigation and Drainage Paper 56. FAO, Rome*, 300  
419 pp.
- 420 Beysens, D., 1995. The formation of dew. *Atmospheric Research*, 39,215–237.
- 421 Beysens, D., Milimouk, I., Nikolayev, V., Muselli, M. Marcillat, J., 2003. Using radiative cooling  
422 to condense atmospheric vapor: a study to improve water yield. *Journal of Hydrology*, 276,  
423 1– 11.
- 424 Beysens, D., Muselli, M., Nikolayev, V., Narhe, R. and Milimouk, I., 2005. Measurement and  
425 modelling of dew in island, coastal and alpine areas *Atmospheric Research*, 73, 1– 22.
- 426 Beysens, D., Clus, O., Mileta, M., Milimouk, I., Musell, M. and Nikolayev, V.S., 2007. Collecting  
427 dew as a water source on small islands: the dew equipment for water project in Bis'evo  
428 (Croatia). *Energy*, 32, 1032–1037.
- 429 Finch, J.W. and Gash, J., 2002. Application of a simple finite difference model for estimating  
430 evaporation from open reservoir. *Journal of hydrology*, 255, 253–259
- 431 Jacobs, F.G.A., Heusinkveld, B.G. and Berkowicz, S.M., 2002. A simple model for potential  
432 dewfall in an arid region. *Atmospheric Research*, 64, 285–295.
- 433 Jacobs, F.G.A., Heusinkveld, B.G. and Berkowicz, S.M., 2008. Passive dew collection in a  
434 grassland area, The Netherlands. *Atmospheric Research*, 87, 377–385.
- 435 Kidron, G.J., 1999. Altitude dependent dew and fog in the Negev Desert, Israel. *Agricultural and*  
436 *Forest Meteorology*, 96, 1–8.
- 437 Kidron, G.J., 2000. Analysis of dew precipitation in three habitats within a small arid drainage  
438 basin, Negev Highlands, Israel. *Atmospheric Research*, 55, 257–270.

- 439 Kidron, G.J., Herrnstadt, I, Barzilay E., 2002. The role of dew as a moisture source for sand  
440 microbiotic crusts in the Negev Desert, Israel. *Journal of Arid Environments*, 52, 517–533
- 441 Lekouch, I., Muselli, M., Kabbachi, B., Ouazzani, J. Melnytchouk-Milimouk, I. and Beysens, D.,  
442 2010. Dew, fog, and rain as supplementary sources of water in south-western Morocco.  
443 *Energy*, 1 – 9. In press, doi:10.1016/j.energy.2010.03.017
- 444 Monteith, J.L., 1957. Dew. *The Quarterly Journal of the Royal Meteorological Society*, 83, 322–  
445 341.
- 446 Moro, M. J., Were, A., Villagarcia , L., Canton, Y. and Domingo, F., 2007. Dew measurement by  
447 Eddy covariance and wetness sensor in a semiarid ecosystem of SE Spain. *Journal of*  
448 *Hydrology*, 335, 295–302.
- 449 Muselli, M., Beysens, D., Marcillat, J., Milimouk, I., Nilsson, T. and Louche, A., 2002. Dew water  
450 collector for potable water in Ajaccio (Corsica island, France). *Atmospheric Research*, 64,  
451 297–312.
- 452 Muselli, M., Beysens, D., Soyeux, E., 2006 (a). Chemical composition of dew water from passive  
453 radiative condenser in Corsica Island (France). *Journal of Environmental Quality* 35,  
454 1812–1817.
- 455 Muselli, M., Beysens, D. and Milimouk, I., 2006 (b). A comparative study of two large radiative  
456 dew water condensers. *Journal of Arid Environments*, 64, 54–76.
- 457 Muselli, M., Beysens, D., Mileta, M. and Milimouk, I., 2009. Dew and rain water collection in the  
458 Dalmatian Coast, Croatia. *Atmospheric Research*, 92, 455–463.
- 459 Nilsson, T.M.J., 1994. Optical scattering properties of pigmented foils for radiative cooling and  
460 water condensation: theory and experiment. Ph.D. Thesis, Department of Physics,  
461 University of Technology, Göteborg, Sweden.
- 462 Richards, K., 2009. Adaptation of a leaf wetness model to estimate dewfall amount on a roof  
463 surface. *Agricultural and Forest Meteorology*, 149, 1377–1383.
- 464 Sharan, G., 2007 (a). Harvesting dew to supplement drinking water supply in arid coastal villages of  
465 Gujarat. Indian Institute of Management. W.P. No. 08–05.

- 466 Sharan, G., Singh S, Clus, O., Milimouk-Melnytchouk, I., Muselli, M., Beysens, D., 2007 (b).  
467           Roofs as Dew Collectors: III. Special Polyethylene Foil on a School in Sayara (NW India).  
468           Proceedings of the 4th Conference on Fog, Fog Collection and Dew (La Serena, Chile),  
469           251–254.
- 470 Sharan, G., Beysens, D. and Milimouk-Melnytchouk, I., 2007 (c). A study of dew water yields on  
471           Galvanized iron roofs in Kothara (North-West India). *Journal of Arid Environments*, 69,  
472           259–269.
- 473 Steinberger, Y., Loboda, I. and Garner, W., 1989. The influence of autumn dewfall on spatial and  
474           temporal distribution of nematodes in the desert ecosystem. *Journal of Arid Environments*,  
475           16, 177–183.
- 476 Vermeulen, A.T., Wyers, G.P., Romer, F.G., Van Leeuwen, N.F.M., Draaijers, G.P.J. and Erisman,  
477           J.W., 1997. Fog deposition on a coniferous forest in the Netherlands. *Atmospheric*  
478           *Environment*, 31, 375–386.



Figure 1. View of the two radiative dew condensers with the black PE foil (BF) and the white standard foil (WSF) fitted to the 30° tilted flat pans.

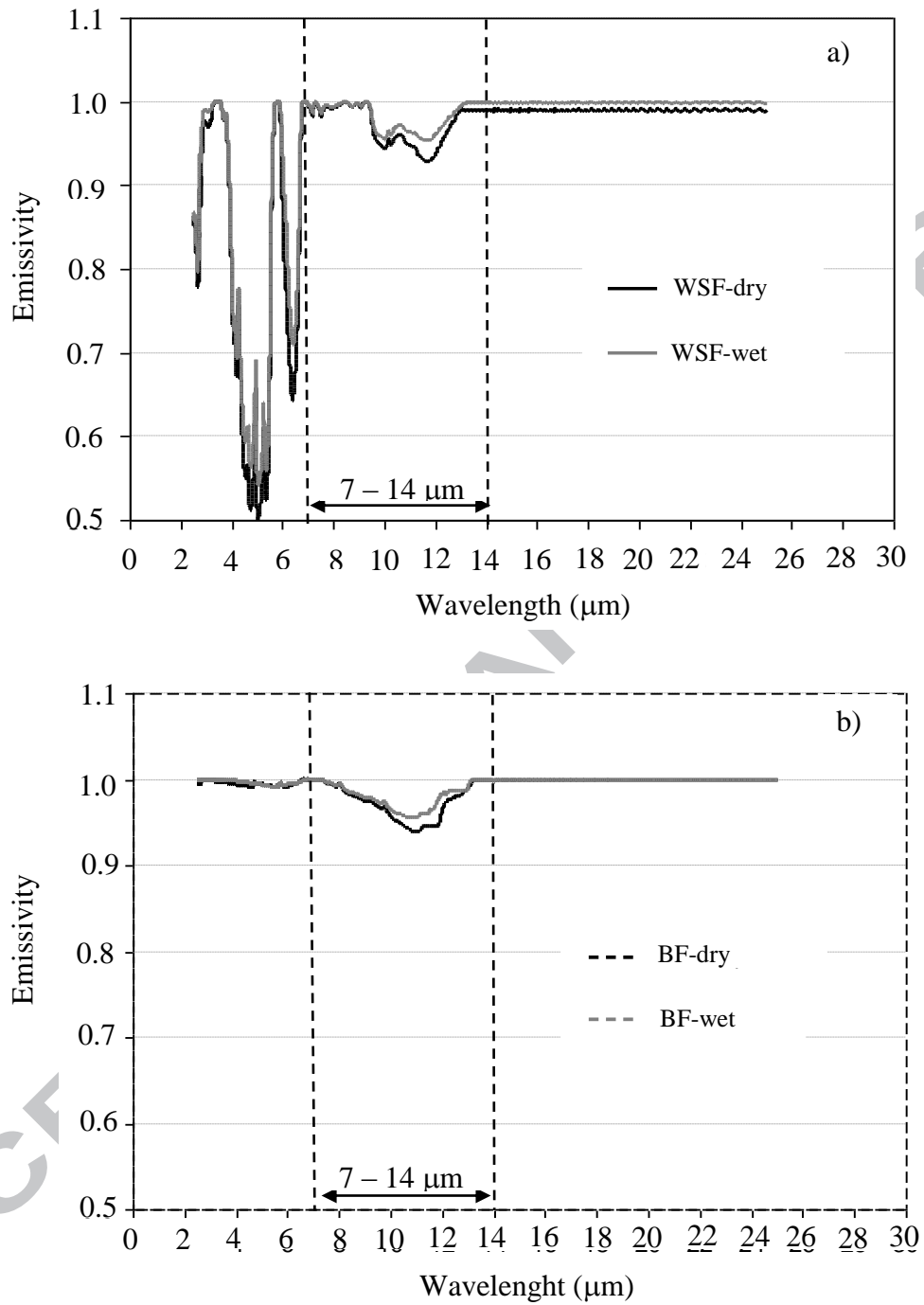


Figure 2. Distribution of the foil emissivity ( $\epsilon$ ) for (a) WSF and (b) BF, under dry and wet conditions in the 2.5-25  $\mu\text{m}$  range. Vertical bars delimit the 7-14  $\mu\text{m}$  region (atmospheric window).

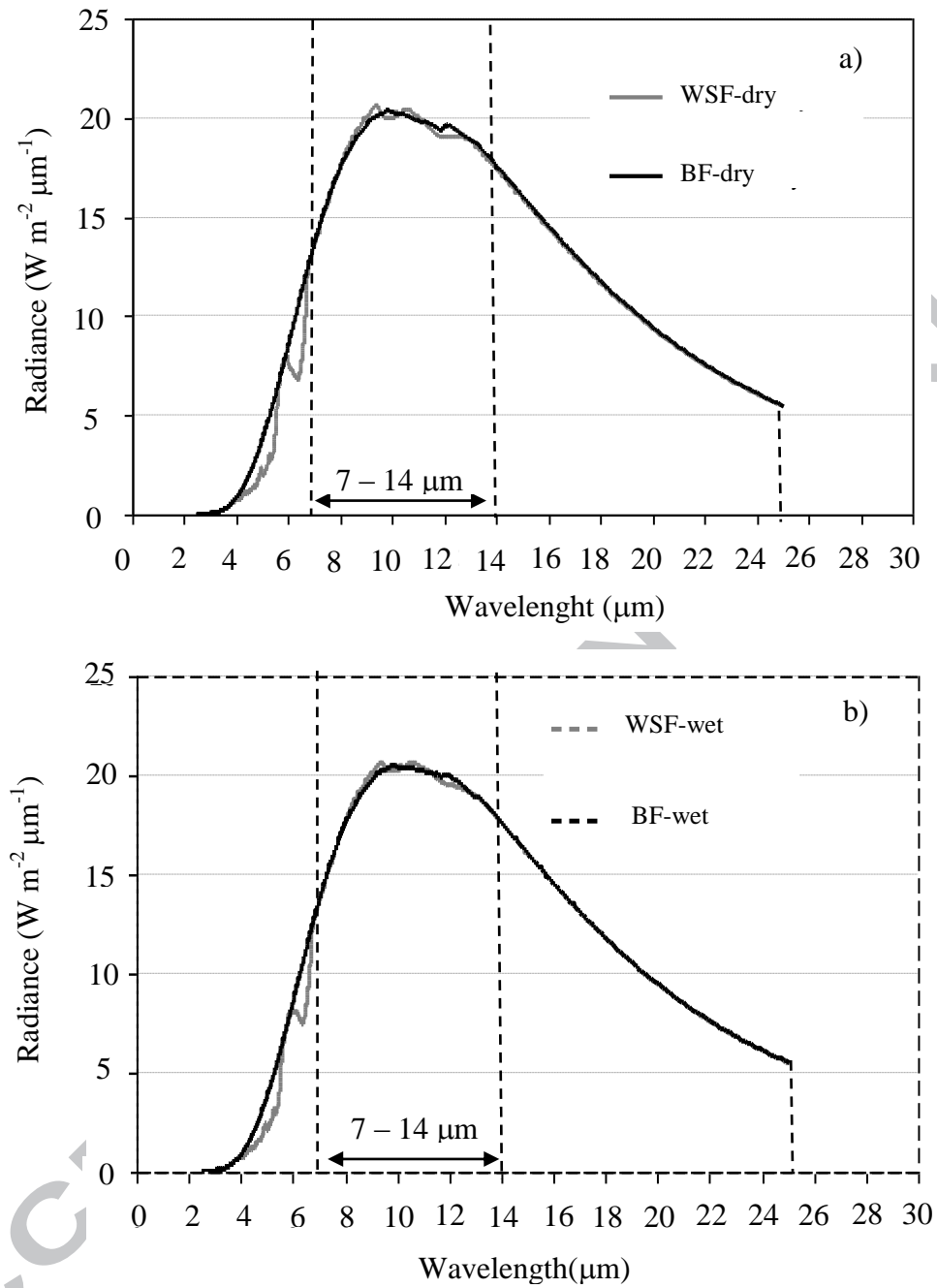


Figure 3. Distribution of emitted radiance ( $W$ ;  $W m^{-2}$ ) in the 2.5-25  $\mu m$  range according to the Planck's law assuming a surface temperature of 278 K for (a) WSF and (b) BF under dry and wet conditions. Vertical bars delimit the 7-14  $\mu m$  region (atmospheric window).

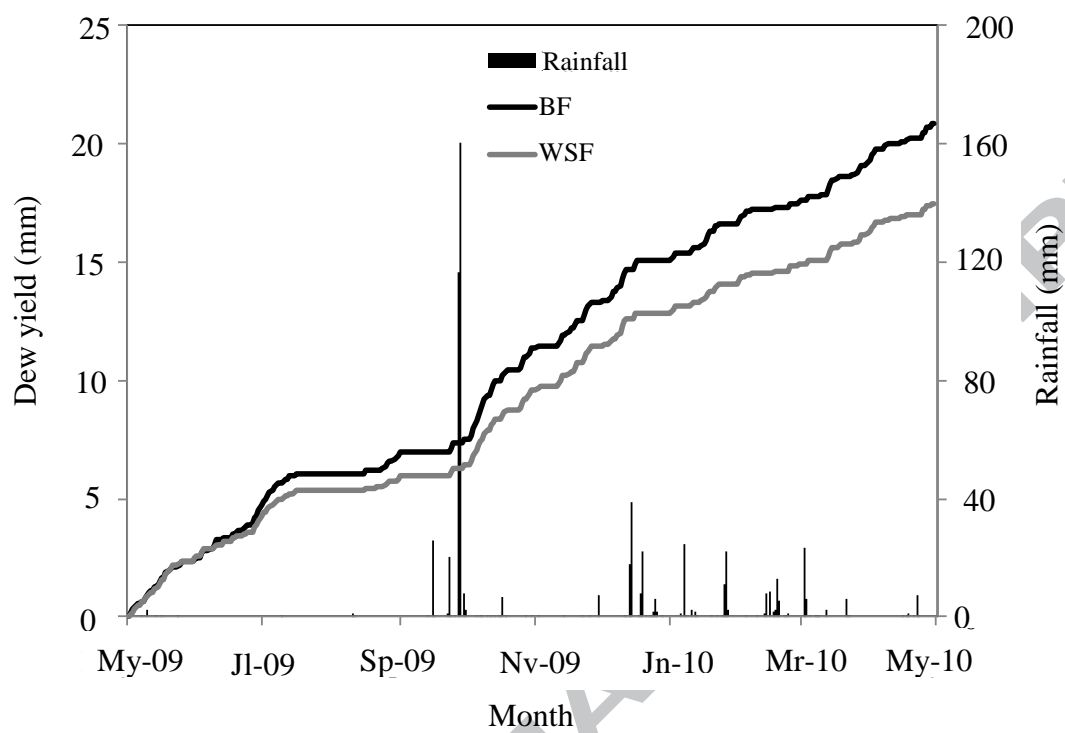


Figure 4. Cumulated dew yield of WSF and BF condensers during the observation period. Bars represent rainfall events (mm).



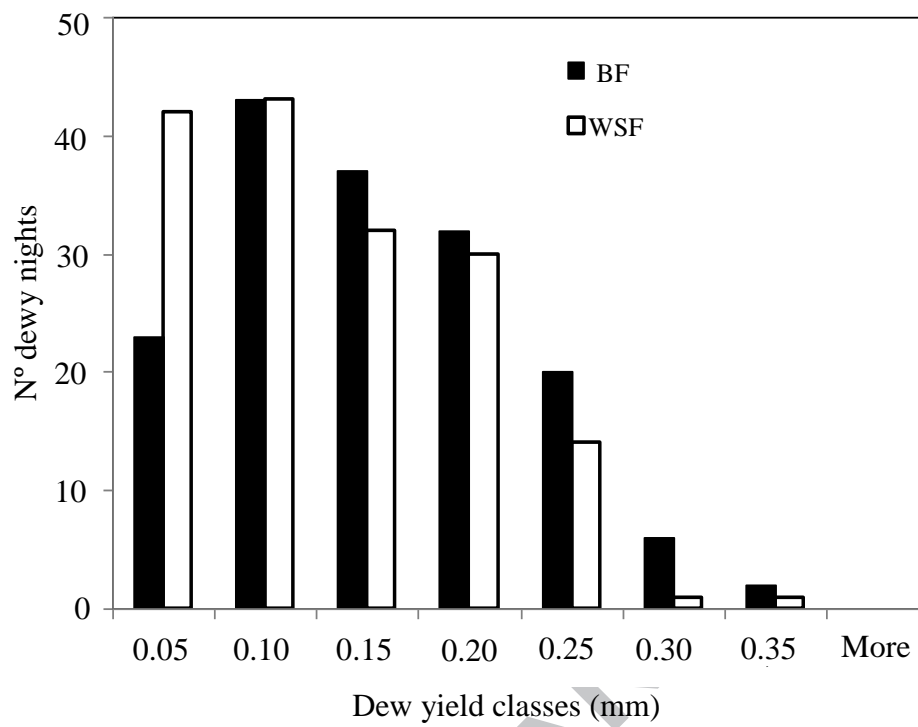


Figure 5. Dew yield frequency histogram of WSF (white bars) and BF (black bars) during the observation period.

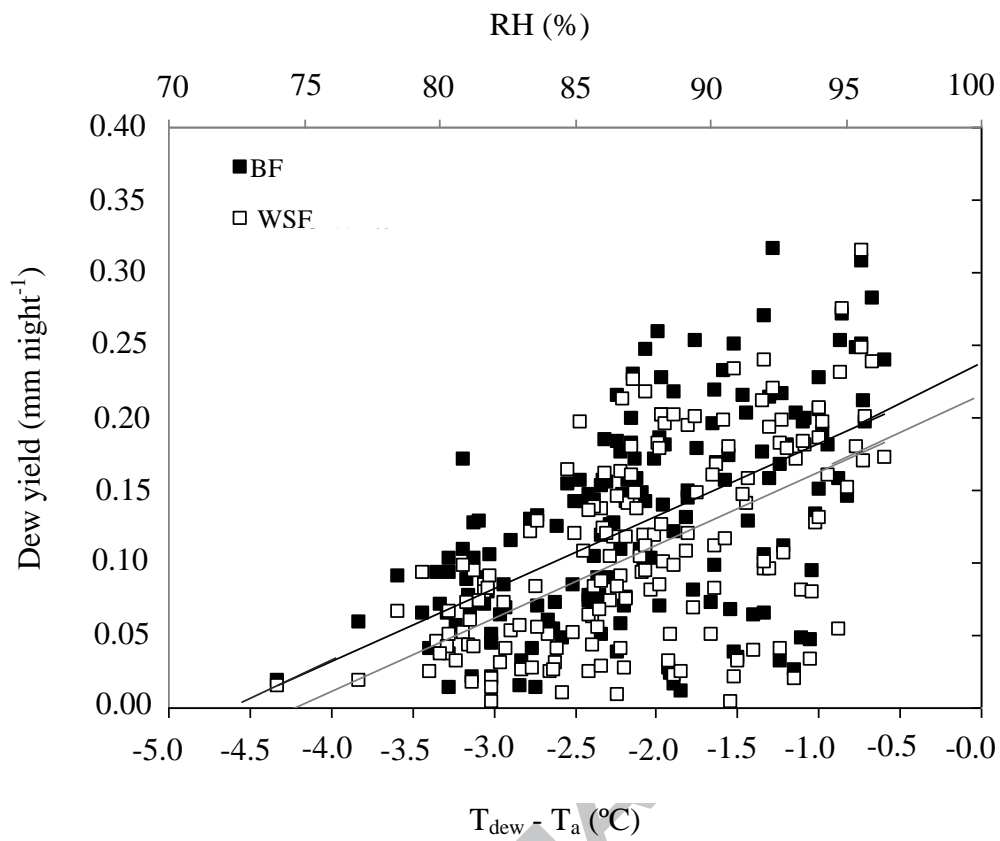


Figure 6. Correlation of dew yield  $Y$  (mm night<sup>-1</sup>) with  $\Delta T = T_{dew} - T_a$  (°C, lower scale) and relative humidity  $RH$  (% , upper scale) for WSF (white symbols) and BF (black symbols).

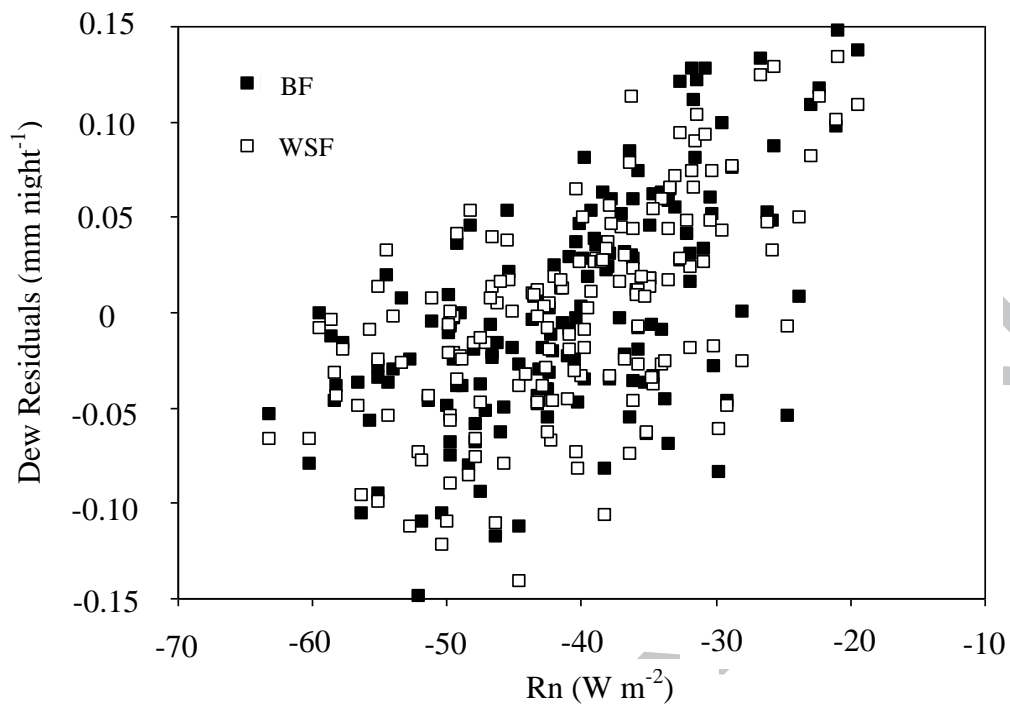


Fig. 7. Relationship between the residuals ( $r$ ) of Eq. (3) and the mean nightly net radiation ( $R_n$ ) for WSF (white symbols) and BF (black symbols).

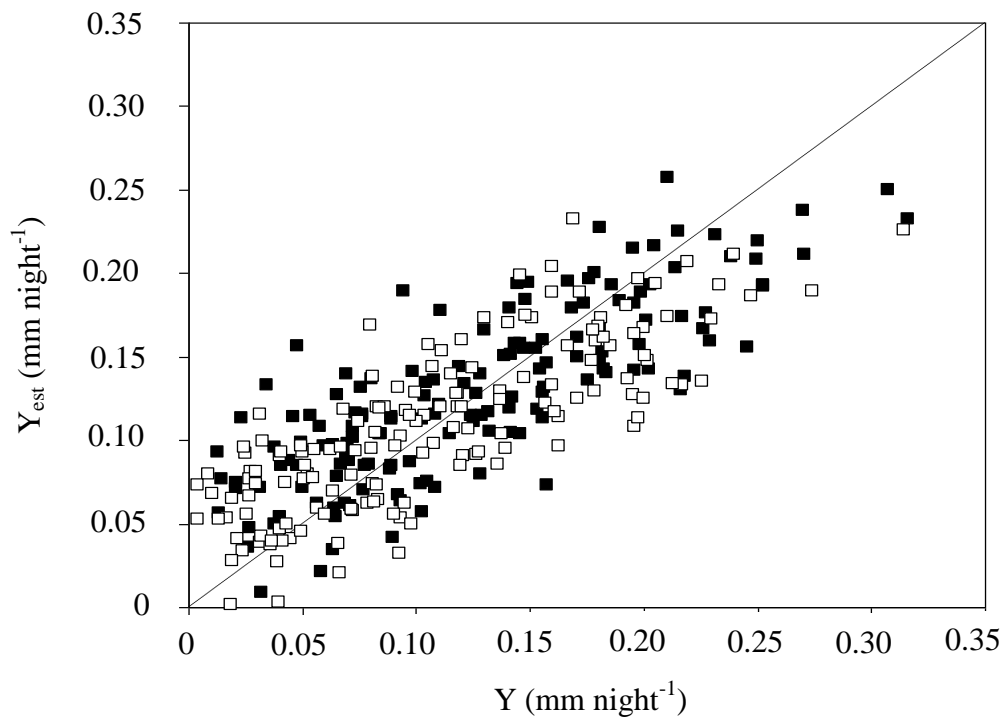


Fig. 8. Comparison between observed ( $Y$ ) and estimated ( $Y_{est}$ ) night dew yield, using Eq. (4) (WSF: white symbols, BF: black symbols). The dashed line is the 1:1 relationship.

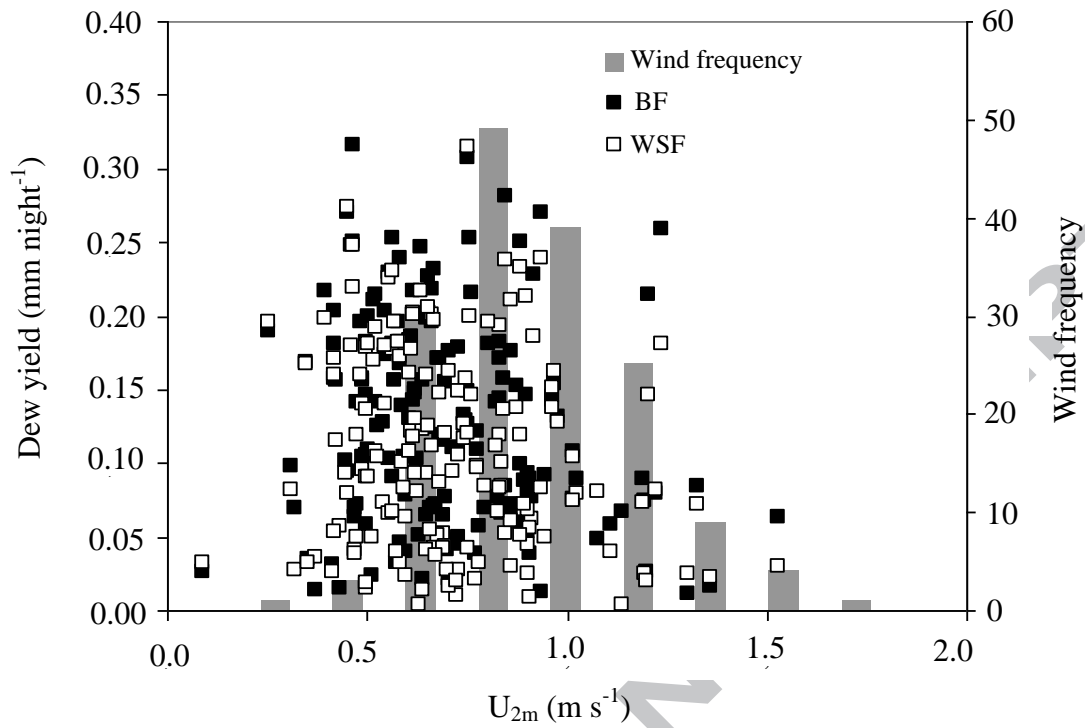


Figure 9. Correlation of dew yield with wind speed  $U_{2m}$  and wind speed frequency classes for WSF (white symbols) and BF (black symbols). Wind frequency has been only plotted for the range where dew formation occurs (0 to 2  $\text{m s}^{-1}$ ).

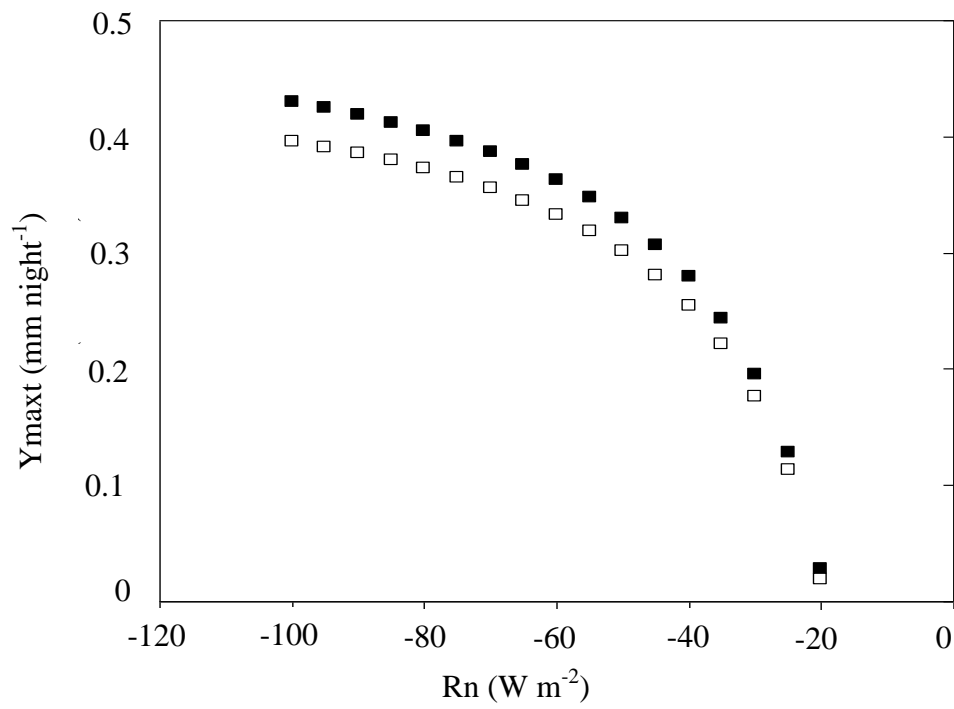


Fig. 10. Maximum dew yield as a function of foil net radiation as predicted from Eq. 5 for WSF (white symbols) and BF (black symbols).

Foil	Condition	Parameters	2.5 - 7 $\mu\text{m}$	7 - 14 $\mu\text{m}$	14 - 25 $\mu\text{m}$	Total MIR
WSF	Dry	$\varepsilon$	0.833	0.976	0.990	0.876
		$\varepsilon^*$	0.825	0.971	0.990	0.971
		$W$	15.4	131.3	115.3	262.0
	Wet	$\varepsilon$	0.854	0.983	0.998	0.893
		$\varepsilon^*$	0.850	0.980	0.998	0.980
		$W$	16.1	132.6	116.3	265.0
BF	Dry	$\varepsilon$	0.996	0.976	0.998	0.992
		$\varepsilon^*$	0.995	0.972	0.998	0.985
		$W$	19.5	131.5	116.3	267.3
	Wet	$\varepsilon$	0.998	0.982	0.999	0.995
		$\varepsilon^*$	0.996	0.980	0.999	0.990
		$W$	19.5	132.5	116.5	268.5

Table 1. Integrated values of emitted radiance ( $W$ ;  $W m^{-2}$ ), emissivity ( $\varepsilon$ ) and radiance-weighted emissivity ( $\varepsilon^*$ ) in the 2.5-7  $\mu\text{m}$ , 7-14  $\mu\text{m}$ , 14 -25  $\mu\text{m}$  and the entire mid-infrared (MIR) ranges under dry and wet conditions.

Year	Month	Number of days				Total dew yield (mm)	
		Dew on WSF	Dew on BF	Rainfall events	Sensor failure	WSF	BF
2009	My	22	22	3	0	2.47	2.43
	Jn	20	19	0	0	1.79	2.29
	Jl*	15	15	0	15	1.06	1.29
	Ag*	10	10	0	12	0.51	0.77
	Sp	6	4	10	0	0.57	0.69
	Oc	20	19	2	0	3.18	3.83
	Nv	17	15	2	0	1.84	1.99
	Dc	13	11	7	0	1.39	1.71
2010	Ja	13	11	7	0	1.12	1.53
	Fb	10	9	9	0	0.87	0.99
	Mr	15	15	7	0	1.30	1.62
	Ap	14	13	3	0	1.26	1.62
Annual		175	163	50	27	17.36	20.76

\*: Months affected by the sensor failure

Table 2. Number of dewy, rainfall and sensor failure nights and total monthly dew yield for the WSF and BF condensers during the observation period.



Month		Dew on WSF			Dew on BF		
		Maximum	Average	Std. Dev.	Maximum	Average	Std. Dev.
2009	M	0.210	0.112	0.060	0.201	0.110	0.051
	Jn	0.226	0.094	0.070	0.246	0.120	0.062
	Jl	0.163	0.070	0.042	0.155	0.086	0.049
	A	0.119	0.050	0.031	0.141	0.077	0.028
	S	0.161	0.143	0.020	0.198	0.174	0.022
	O	0.237	0.167	0.051	0.316	0.201	0.061
	N	0.274	0.123	0.081	0.270	0.133	0.079
	D	0.314	0.127	0.089	0.307	0.155	0.091
2010	Ja	0.172	0.107	0.051	0.238	0.139	0.070
	F	0.213	0.096	0.070	0.215	0.111	0.058
	M	0.205	0.086	0.066	0.231	0.108	0.069
	A	0.233	0.092	0.059	0.250	0.124	0.072
Annual		0.314	0.105	0.031	0.316	0.128	0.035

Std. Dev.: Standard Deviation

Table 3. Monthly and annual maximum, average, and standard deviation of dew yield for the WSF and BF condensers during the observation period.

(i) Eq. 3: $Y_{\text{est}} = a_1((T_d - T_a) + a_2)$	WSF	BF
$a_1$ (mm night <sup>-1</sup> °C <sup>-1</sup> )	0.049 ± 0.005	0.051 ± 0.006
$a_2$ (C <sup>-1</sup> )	-4.2 ± 0.260	-4.6 ± 0.297
$R^2$	0.33	0.32
RMSE (mm night <sup>-1</sup> )	0.043	0.045
MBE (mm night <sup>-1</sup> )	0.003	0.003
(ii) Eq. 4: $Y_{\text{est}} = b_1((T_d - T_a) + b_2) (1 + b_3/R_n)$		
$b_1$ (mm night <sup>-1</sup> °C <sup>-1</sup> )	0.126 ± 0.011	0.129 ± 0.011
$b_2$ (C <sup>-1</sup> )	3.9 ± 0.128	4.1 ± 0.137
$b_3$ (W m <sup>-2</sup> )	19,21 ± 0.94	18.93 ± 0.88
$R^2$	0.63	0.65
RMSE (mm night <sup>-1</sup> )	0.035	0.035
MBE (mm night <sup>-1</sup> )	0.002	0.002

Table 4. Values of (i) fitted parameters and (ii) statistical parameters characterizing the predictive performance for Eqs. 3 and 4

479

480 **Research highlights**

- 481 • We compare the performance of two polyethylene foil materials for dew harvesting.
- 482 • Dew was well correlated with the air relative humidity and foil net radiation.
- 483 • Black foil (BF) was more productive.
- 484 • Surface emissivity and hydrophilic properties are two key parameters.
- 485 • Our empirical relationship explained about two-thirds of the total variance of dew.

486

487

ACCEPTED MANUSCRIPT